

FERMI NATIONAL ACCELERATOR LABORATORY

FERMILAB-TM-XXXX-E
TEVEWWG/top 2013/xx
CDF Note 10976
DØ Note 6381
March 2013

Combination of CDF and DØ results on the mass of the top quark using up to 8.7 fb^{-1} of $p\bar{p}$ collisions.

The Tevatron Electroweak Working Group¹
for the CDF and DØ Collaborations

Abstract

We summarize the top-quark mass measurements from the CDF and DØ experiments at Fermilab. We combine published Run I (1992–1996) measurements with the most precise published and preliminary Run II (2001–2012) measurements using a data set corresponding to up to 8.7 fb^{-1} of $p\bar{p}$ collisions. Taking correlations of uncertainties into account, and adding in quadrature the statistical and systematic uncertainties, the resulting preliminary Tevatron average mass of the top quark is $M_t = 173.20 \pm 0.87 \text{ GeV}/c^2$.

¹The Tevatron Electroweak Working Group can be contacted at tev-ewwg@fnal.gov.
More information can be found at <http://tevewwg.fnal.gov>.

1 Introduction

This note reports the Tevatron average top-quark mass obtained by combining the most precise published and preliminary measurements of the top-quark mass. The ATLAS and CMS collaborations have also performed a combination of their most recent top quark mass measurements [1].

The CDF and DØ collaborations have performed several direct experimental measurements of the top-quark mass (M_t) using data collected at the Tevatron proton-antiproton collider located at the Fermi National Accelerator Laboratory. These pioneering measurements were first based on approximately 0.1 fb^{-1} of Run I data [1–12] collected from 1992 to 1996, and included results from the decay channels $t\bar{t} \rightarrow W^+bW^-\bar{b} \rightarrow qq'bqq'\bar{b}$ (alljets), $t\bar{t} \rightarrow W^+bW^-\bar{b} \rightarrow \ell\nu bqq'\bar{b}$ (ℓ +jets)², and $t\bar{t} \rightarrow W^+bW^-\bar{b} \rightarrow \ell^+\nu b\ell^-\bar{\nu}\bar{b}$ ($\ell\ell$). Since the combination performed in 2011 [14] a new final state signature was introduced by CDF, which requires events to possess missing transverse energy (\cancel{E}_T) and jets, but no identified lepton (labeled MET) [15, 16]. This sample is statistically independent from the previously mentioned three channels and is considered a fourth.

The Run II (2001–2011) measurements considered here are the most recent results in these channels, using up to 8.7 fb^{-1} of data, corresponding to the full Run II dataset for CDF [15, 17, 18, 19, 20, 21, 22]. The CDF analysis using charged particle tracking (L_{XY}/p_T^{lep}) uses a data set corresponding to a luminosity of 1.9 fb^{-1} [23]. There are no plans to update this analysis.

With respect to the July 2011 combination [14] and the published version of the combination [24], the Run II CDF measurement in the ℓ +jets channel has been updated using 8.7 fb^{-1} of data, an improved analysis technique, and improved jet energy resolution [17]. The CDF measurement in the MET channel was updated with 8.7 fb^{-1} of data as well [15]. The now published Run II CDF measurements in the $\ell\ell$ channel [18] and alljets channel [19] are unchanged. The measurement based on charged particle tracking [23] was incorporated as described in the past combinations [14]. The corresponding sample has been split into the decay length significance L_{XY} and lepton transverse momentum p_T^{lep} parts and the latter was removed from the combination due to statistical correlation with other samples.

The DØ Run II measurements presented in this note include the most recent Run II measurement in the $\ell\ell$ [22] channel using 5.4 fb^{-1} of data and in the ℓ +jets channel [21] with 3.6 fb^{-1} of data. Both results are now published.

The Tevatron average top-quark mass is obtained by combining five published Run I measurements [3, 4, 6, 8, 11, 12] with four published Run II CDF results [17, 18, 19, 23] results,

²Here $\ell = e$ or μ . Decay channels with explicit tau lepton identification are presently under study and are not yet used for measurements of the top-quark mass. Decays with $\tau \rightarrow e, \mu$ are included in the direct $W \rightarrow e$ and $W \rightarrow \mu$ channels.

35 one preliminary Run II CDF result [15], and two published Run II DØ results [21, 22]. This
36 combination supersedes previous combinations [14, 25, 26, 27, 28, 29, 30, 31, 32, 33].

37 The definition and evaluation of the systematic uncertainties and the understanding of the
38 correlations among channels, experiments, and Tevatron runs is the outcome of many years of
39 joint work between the CDF and DØ collaborations and is described in detail elsewhere [24].

40 The input measurements and uncertainty categories used in the combination are detailed
41 in Sections 2 and 3, respectively. The correlations assumed in the combination are discussed in
42 Section 4 and the resulting Tevatron average top-quark mass is given in Section 5. A summary
43 and future plans are presented in Section 6.

44 2 Input Measurements

45 Twelve measurements of M_t used in this combination are reported in Table 1. The Run I mea-
46 surements all have relatively large statistical uncertainties and their systematic uncertainties
47 are dominated by the total jet energy scale (JES) uncertainty. In Run II both CDF and DØ
48 take advantage of the larger $t\bar{t}$ samples available and employ new analysis techniques to reduce
49 both of these uncertainties. In particular, the Run II DØ analysis in the ℓ +jets channel and the
50 Run II CDF analyses in the ℓ +jets, alljets, and MET channels constrain the response of light-
51 quark jets using the kinematic information from $W \rightarrow qq'$ decays (so-called *in situ* calibration).
52 Residual JES uncertainties associated with p_T and η dependencies as well as uncertainties spe-
53 cific to the response of b -jets are treated separately. The Run II DØ $\ell\ell$ measurement uses the
54 JES determined in the ℓ +jets channel by *in situ* calibration.

55 The DØ Run II ℓ +jets analysis uses the JES determined from the external calibration
56 derived from γ +jets events as an additional Gaussian constraint to the *in situ* calibration.
57 Therefore, the total resulting JES uncertainty is split into one part emerging from the *in*
58 *situ* calibration and another part emerging from the external calibration. To do that, the
59 measurement without external JES constraint has been combined iteratively with a pseudo-
60 measurement using the method of Refs. [34, 35] which uses only the external calibration in a
61 way that the combination give the actual total JES uncertainty. The splitting obtained in this
62 way is used to assess both the statistical part of the JES uncertainty and the part of the JES
63 uncertainty coming from the external calibration constraint [36].

64 The L_{XY} technique developed by CDF uses the decay length of B-mesons from b -tagged
65 jets. While the statistical sensitivity of this analysis is not as good as for the more traditional
66 methods, this technique has the advantage that since it uses primarily tracking information, it
67 is almost entirely independent of JES uncertainties.

68 The DØ Run II ℓ +jets result is a combination of the published Run IIa (2002–2005) mea-

Table 1: Summary of the measurements used to determine the Tevatron average M_t . Integrated luminosity ($\int \mathcal{L} dt$) has units of fb^{-1} , and all other numbers are in GeV/c^2 . The uncertainty categories and their correlations are described in Section 3. The total systematic uncertainty and the total uncertainty are obtained by adding the relevant contributions in quadrature. “n/a” stands for “not applicable”, “n/e” for “not evaluated”.

March 2013

	Run I published					Run II published					Run II preliminary	
	CDF			DØ		CDF				DØ		CDF
$\int \mathcal{L} dt$	ℓ +jets	$\ell\ell$	alljets	ℓ +jets	$\ell\ell$	ℓ +jets	$\ell\ell$	alljets	Lxy	ℓ +jets	$\ell\ell$	MEt
	0.1	0.1	0.1	0.1	0.1	8.7	5.6	5.8	1.9	3.6	5.3	8.7
Result	176.1	167.4	86.0	180.1	168.4	172.85	170.28	172.47	166.90	174.94	174.00	173.95
In situ light-jet calibration (iJES)	n/a	n/a	n/a	n/a	n/a	0.49	n/a	0.95	n/a	0.53	0.55	1.05
Response to $b/q/g$ jets (aJES)	n/a	n/a	n/a	0.0	0.0	0.09	0.14	0.03	n/a	0.0	0.40	0.10
Model for b jets (bJES)	0.6	0.8	0.6	0.7	0.7	0.16	0.33	0.15	n/a	0.07	0.20	0.17
Out-of-cone correction (cJES)	2.7	2.6	3.0	2.0	2.0	0.21	2.13	0.24	0.36	n/a	n/a	0.18
Light-jet response (2) (dJES)	0.7	0.6	0.3	2.5	1.1	0.07	0.58	0.04	0.06	0.63	0.56	0.04
Light-jet response (1) (rJES)	3.4	2.7	4.0	n/a	n/a	0.48	2.01	0.38	0.24	n/a	n/a	0.40
Lepton modeling (LepPt)	n/e	n/e	n/e	n/e	n/e	0.03	0.27	n/a	n/a	0.17	0.35	n/a
Signal modeling (Signal)	2.6	2.9	2.0	1.1	1.8	0.61	0.73	0.62	0.90	0.77	0.86	0.64
Jet modeling (DetMod)	0.0	0.0	0.0	0.0	0.0	0.0	0.0	0.0	0.0	0.36	0.50	0.0
Offset (UN/MI)	n/a	n/a	n/a	1.3	1.3	n/a	n/a	n/a	n/a	n/a	n/a	n/a
Background from theory (BGMC)	1.3	0.3	1.7	1.0	1.1	0.12	0.24	0.0	0.80	0.18	0.0	0.0
Background based on data (BGData)	0.0	0.0	0.0	0.0	0.0	0.16	0.14	0.56	0.20	0.23	0.20	0.12
Calibration method (Method)	0.0	0.7	0.6	0.6	1.1	0.00	0.12	0.38	2.50	0.16	0.51	0.31
Multiple interactions model (MHI)	n/e	n/e	n/e	n/e	n/e	0.07	0.23	0.08	0.0	0.05	0.0	0.18
Systematic uncertainty (Syst)	5.3	4.9	5.7	3.9	3.6	0.98	3.09	1.49	2.90	1.24	1.44	1.35
Statistical uncertainty (Stat)	5.1	10.3	10.0	3.6	12.3	0.52	1.95	1.43	9.00	0.83	2.36	1.26
Total uncertainty	7.3	11.4	11.5	5.3	12.8	1.11	3.79	2.06	9.46	1.50	2.76	1.85

69 surement [20] with 1 fb^{-1} of data and the result obtained with 2.6 fb^{-1} of data from Run IIb
70 (2006–2007) [21]. This analysis includes an additional particle response correction on top of
71 the standard *in-situ* calibration. The DØ Run II $\ell\ell$ result is based on a neutrino weighting
72 technique using 5.4 fb^{-1} of Run II data [22].

73 Table 1 also lists the individual uncertainties of each result, subdivided into the categories
74 described in the next Section. The correlations between the inputs are described in Section 4.

75 3 Uncertainty Categories

76 We employ uncertainty categories similar to what was used for the previous Tevatron aver-
77 age [14, 24], with small modifications to better account for their correlations. They are divided
78 such that sources of systematic uncertainty that share the same or similar origin are combined
79 as explained in [24]. For example, the “Signal modeling” (“Signal”) category discussed below
80 includes the uncertainties from different systematic sources which are correlated due to their
81 origin in the modeling of the simulated signal samples.

82 Some systematic uncertainties have been separated into multiple categories in order to ac-
83 commodate specific types of correlations. For example, the jet energy scale (JES) uncertainty
84 is subdivided into six components in order to more accurately accommodate our best under-
85 standing of the relevant correlations between input measurements.

86 For this note we use the new systematic naming scheme described in [24]. In parentheses,
87 the old names of the systematic uncertainties are provided. There is a one-to-one matching
88 between the new and old systematic definitions of categories.

89 **Statistical uncertainty (Statistics):** The statistical uncertainty associated with the M_t de-
90 termination.

91 **In situ light-jet calibration (iJES):** That part of the JES uncertainty which originates
92 from *in situ* calibration procedures and is uncorrelated among the measurements. In
93 the combination reported here, it corresponds to the statistical uncertainty associated
94 with the JES determination using the $W \rightarrow qq'$ invariant mass in the CDF Run II ℓ +jets,
95 alljets, and MET measurements and the DØ Run II ℓ +jets measurement. It also includes
96 for the DØ Run II ℓ +jets measurement the uncertainty coming from the MC/data dif-
97 ference in jet response that is uncorrelated with the other DØ Run II measurements.
98 Residual JES uncertainties arising from effects not considered in the *in situ* calibration
99 are included in other categories.

100 **Response to $b/q/g$ jets (aJES):** That part of the JES uncertainty which originates from
101 differences in detector electromagnetic over hadronic (e/h) response between b -jets and
102 light-quark jets.

103 **Model for b jets (bJES):** That part of the JES uncertainty which originates from uncer-
104 tainties specific to the modeling of b -jets and which is correlated across all measurements.
105 For both CDF and DØ this includes uncertainties arising from variations in the semilep-
106 tonic branching fractions, b -fragmentation modeling, and differences in the color flow
107 between b -jets and light-quark jets. These were determined from Run II studies but back-
108 propagated to the Run I measurements, whose *Light-jet response (1)* uncertainties (*rJES*,
109 see below) were then corrected in order to keep the total JES uncertainty constant.

110 **Out-of-cone correction (cJES):** That part of the JES uncertainty which originates from
111 modeling uncertainties correlated across all measurements. It specifically includes the
112 modeling uncertainties associated with light-quark fragmentation and out-of-cone correc-
113 tions. For $D\bar{O}$ Run II measurements, it is included in the *Light-jet response (2) (dJES)*
114 category.

115 **Light-jet response (1) (rJES):** The remaining part of the JES uncertainty which is corre-
116 lated between all measurements of the same experiment independently from the data-
117 taking period, but which is uncorrelated between experiments. It is specific to CDF and
118 is dominated by uncertainties in the calorimeter response to light-quark jets, and also in-
119 cludes small uncertainties associated with the multiple interaction and underlying event
120 corrections.

121 **Light-jet response (2) (dJES):** That part of the JES uncertainty which originates from
122 limitations in the data samples used for calibrations and which is correlated between
123 measurements within the same data-taking period, such as Run I or Run II, but not
124 between experiments. For CDF this corresponds to uncertainties associated with the
125 η -dependent JES corrections which are estimated using di-jet data events. For $D\bar{O}$ this
126 includes uncertainties in the calorimeter response for light jets, uncertainties from p_T -
127 and η -dependent JES corrections and from the sample dependence of using γ +jets data
128 samples to derive the JES.

129 **Lepton modeling (LepPt):** The systematic uncertainty arising from uncertainties in the
130 scale of lepton transverse momentum measurements. It was not considered as a source of
131 systematic uncertainty in the Run I measurements.

132 **Signal modeling (Signal):** The systematic uncertainty arising from uncertainties in $t\bar{t}$ mod-
133 eling that is correlated across all measurements. This includes uncertainties from vari-
134 ations of the amount of initial and final state radiation and from the choice of parton
135 density function used to generate the $t\bar{t}$ Monte Carlo samples that calibrate each method.
136 For $D\bar{O}$, it also includes the uncertainty from higher order corrections evaluated from a
137 comparison of $t\bar{t}$ samples generated by MC@NLO [37] and ALPGEN [38], both inter-
138 faced to HERWIG [39, 40] for the simulation of parton showers and hadronization. In
139 this combination, the systematic uncertainty arising from a variation of the phenomeno-
140 logical description of color reconnection (CR) between final state particles [41, 42] is
141 included in the *Signal modeling* category. The CR uncertainty is obtained taking the
142 difference between the PYTHIA 6.4 tune “Apro” and the PYTHIA 6.4 tune “ACRpro”
143 that differ only in the color reconnection model. This uncertainty was not evaluated in
144 Run I since the Monte Carlo generators available at that time did not allow varying the
145 CR model. These measurements therefore do not include this source of systematic uncer-
146 tainty. Finally, the systematic uncertainty associated with variations of the physics model
147 used to calibrate the mass extraction method is added. It includes variations observed
148 when substituting PYTHIA [43, 44, 45] (Run I and Run II) or ISAJET [46] (Run I) for
149 HERWIG [39, 40] when modeling the $t\bar{t}$ signal.

150 **Jet modeling (DetMod):** The systematic uncertainty arising from uncertainties in the mod-
151 eling of the detector in the MC simulation. For $D\bar{O}$ this includes uncertainties from jet
152 resolution and identification. CDF found these effects to have a negligible contributions
153 to the measured mass.

154 **Background from theory (BGMC):** Background from theory (MC) takes into account the
155 uncertainty in modeling the background sources. It is correlated between all measure-
156 ments in the same channel, and includes uncertainties on the background composition
157 and on normalization and shape of different components, e.g., the uncertainties from the
158 modeling of the W +jets background in the ℓ +jets channel associated with variations of
159 the factorization scale used to simulate W +jets events.

160 **Background based on data (BGData):** This includes uncertainties associated with the mod-
161 eling using data of the QCD multijet backgrounda in the alljets, MET, and ℓ +jets channels
162 and the Drell-Yan background in the $\ell\ell$ channel evaluated. This part is uncorrelated be-
163 tween experiments.

164 **Calibration method (Method):** The systematic uncertainty arising from any source specific
165 to a particular fit method, including the finite Monte Carlo statistics available to calibrate
166 each method.

167 **Offset (UN/MI):** This is specific to $D\bar{O}$ and includes the uncertainty arising from uranium
168 noise in the $D\bar{O}$ calorimeter and from the multiple interaction corrections to the JES.
169 For $D\bar{O}$ Run I these uncertainties were sizable, while for Run II, owing to the shorter
170 calorimeter electronics integration time and *in situ* JES calibration, these uncertainties
171 are negligible.

172 **Multiple interactions model (MHI):** The systematic uncertainty arising from a mismod-
173 eling of the distribution of the number of collisions per Tevatron bunch crossing owing
174 to the steady increase in the collider instantaneous luminosity during data-taking. This
175 uncertainty has been separated from other sources to account for the fact that it is un-
176 correlated between experiments.

177 These categories represent the current preliminary understanding of the various sources of
178 uncertainty and their correlations. We expect these to evolve as we continue to probe each
179 method's sensitivity to the various systematic sources with ever improving precision.

180 4 Correlations

181 The following correlations are used for the combination:

Table 2: The matrix of correlation coefficients used to determine the Tevatron average top-quark mass.

March 2013

	Run I published					Run II published					Run II preliminary CDF MEt	
	CDF			D ϕ		CDF				D ϕ		
	ℓ +jets	$\ell\ell$	alljets	ℓ +jets	$\ell\ell$	ℓ +jets	$\ell\ell$	alljets	L_{XY}	ℓ +jets		$\ell\ell$
CDF-I ℓ +jets	1.00	0.29	0.32	0.26	0.11	0.49	0.54	0.25	0.07	0.21	0.12	0.27
CDF-I $\ell\ell$	0.29	1.00	0.19	0.15	0.08	0.29	0.32	0.15	0.04	0.13	0.08	0.17
CDF-I alljets	0.32	0.19	1.00	0.14	0.07	0.30	0.38	0.15	0.04	0.09	0.06	0.16
D ϕ -I ℓ +jets	0.26	0.15	0.14	1.00	0.16	0.22	0.27	0.12	0.05	0.14	0.07	0.12
D ϕ -I $\ell\ell$	0.11	0.08	0.07	0.16	1.00	0.11	0.13	0.07	0.02	0.07	0.05	0.07
CDF-II ℓ +jets	0.49	0.29	0.30	0.22	0.11	1.00	0.48	0.29	0.08	0.30	0.18	0.33
CDF-II $\ell\ell$	0.54	0.32	0.38	0.27	0.13	0.48	1.00	0.25	0.06	0.11	0.07	0.26
CDF-II alljets	0.25	0.15	0.15	0.12	0.07	0.29	0.25	1.00	0.04	0.16	0.10	0.17
CDF-II L_{XY}	0.07	0.04	0.04	0.05	0.02	0.08	0.06	0.04	1.00	0.06	0.03	0.04
D ϕ -II ℓ +jets	0.21	0.13	0.09	0.14	0.07	0.30	0.11	0.16	0.06	1.00	0.39	0.18
D ϕ -II $\ell\ell$	0.12	0.08	0.06	0.07	0.05	0.18	0.07	0.10	0.03	0.39	1.00	0.11
CDF-II MEt	0.27	0.17	0.16	0.12	0.07	0.33	0.26	0.17	0.04	0.18	0.11	1.00

- 182 • The uncertainties in the *Statistical uncertainty (Stat)*, *Calibration method (Method)*, and
183 *In situ light-jet calibration (iJES)* categories are taken to be uncorrelated among the
184 measurements.
- 185 • The uncertainties in the *Response to b/q/g jets (aJES)*, *Light-jet response (2) (dJES)*,
186 *Lepton modeling (LepPt)*, and *Multiple interactions model (MHI)* categories are taken
187 to be 100% correlated among all Run I and all Run II measurements within the same
188 experiment, but uncorrelated between Run I and Run II and uncorrelated between the
189 experiments.
- 190 • The uncertainties in the *Light-jet response (1) (rJES)*, *Jet modeling (DetMod)*, and *Offset*
191 *(UN/MI)* categories are taken to be 100% correlated among all measurements within the
192 same experiment but uncorrelated between the experiments.
- 193 • The uncertainties in the *Backgrounds estimated from theory (BGMC)* category are taken
194 to be 100% correlated among all measurements in the same channel.
- 195 • The uncertainties in the *Backgrounds estimated from data (BGData)* category are taken
196 to be 100% correlated among all measurements in the same channel and same run period,
197 but uncorrelated between the experiments.
- 198 • The uncertainties in the *Model for b jets (bJES)*, *Out-of-cone correction (cJES)* and *Signal*
199 *modeling (Signal)* categories are taken to be 100% correlated among all measurements.

200 Using the inputs from Table 1 and the correlations specified here, the resulting matrix of total
201 correlation coefficients is given in Table 2.

202 The measurements are combined using a program implementing two independent meth-
203 ods: a numerical χ^2 minimization and the analytic best linear unbiased estimator (BLUE)

204 method [34, 35]. The two methods are mathematically equivalent. It has been checked that
 205 they give identical results for the combination. The BLUE method yields the decomposition of
 206 the uncertainty on the Tevatron M_t average in terms of the uncertainty categories specified for
 207 the input measurements [35].

208 5 Results

209 The combined value for the top-quark mass is: $M_t = 173.20 \pm 0.51$ (stat) ± 0.71 (syst) GeV/ c^2 .
 210 Adding the statistical and systematic uncertainties in quadrature yields a total uncertainty of
 211 0.87 GeV/ c^2 , corresponding to a relative precision of 0.50% on the top-quark mass. It has a
 212 χ^2 of 8.5 for 11 degrees of freedom, corresponding to a probability of 67%, indicating good
 213 agreement among all input measurements. The breakdown of the uncertainties is shown in
 214 Table 3. The total statistical and systematic uncertainties are slightly smaller than in the
 215 Summer 2011 combination [14] and the published combination [24] due to the increase of the
 216 CDF data samples in the ℓ +jets and MET analyses and better treatment of JES corrections in
 217 the ℓ +jets analysis.

218 The pull and weight for each of the inputs are listed in Table 4. The input measurements
 219 and the resulting Tevatron average mass of the top quark are summarized in Fig. 1.

220 The weights of some of the measurements are negative, occurs if the correlation between
 221 two measurements is larger than the ratio of their total uncertainties. In these instances the
 222 less precise measurement will acquire a negative weight. While a weight of zero means that
 223 a particular input is effectively ignored in the combination, a negative weight means that it
 224 affects the resulting M_t central value and helps reduce the total uncertainty. To visualize the
 225 weight each measurement carries in the combination, Fig. 2 shows the absolute values of the
 226 weight of each measurement divided by the sum of the absolute values of the weights of all
 227 input measurements.

228 No input has an anomalously large pull and the χ^2 from the combination of all measure-
 229 ments, which indicates that there is good agreement among them. It is, however, still interesting
 230 to also determine the top-quark mass in the alljets, ℓ +jets, $\ell\ell$, and MET channels. We use the
 231 same methodology, inputs, uncertainty categories, and correlations as described above, but fit
 232 the four physical observables, M_t^{alljets} , M_t^{1+j} , $M_t^{\text{di-1}}$, and M_t^{MET} separately. The results of these
 233 combinations are shown in Table 5.

234 Using the expression in ³ and the results of Table 5 we calculate the following chi-squares
 235 $\chi^2(\ell + \text{jets} - \ell\ell) = 1.30/1$, $\chi^2(\ell + \text{jets} - \text{alljets}) = 0.07/1$, $\chi^2(\ell + \text{jets} - \text{MET}) = 0.11/1$,
 236 $\chi^2(\ell\ell - \text{alljets}) = 0.42/1$, $\chi^2(\ell\ell - \text{MET}) = 1.22/1$ and $\chi^2(\text{alljets} - \text{MET}) = 0.19/1$. These

³For two measurements, x and y , we calculate their consistency using $\chi^2 = (x - y)^2 / \sigma_{x-y}^2$, where $\sigma_{x-y}^2 = \sigma_x^2 + \sigma_y^2 - 2\rho_{xy}\sigma_x\sigma_y$, where ρ_{xy} is the (x, y) correlation coefficient.

Mass of the Top Quark

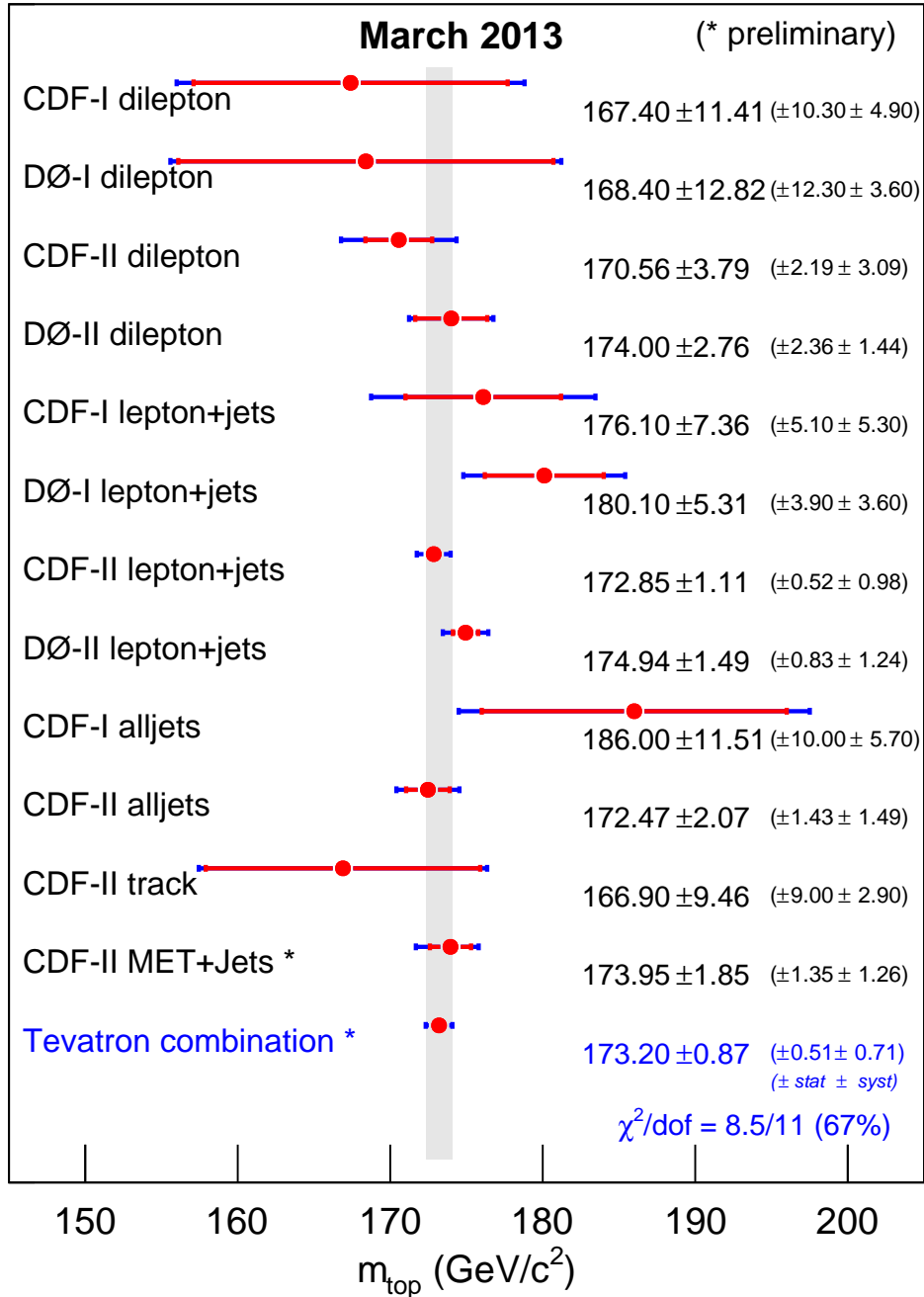


Figure 1: Summary of the input measurements and resulting Tevatron average mass of the top-quark. The results from different measurements are rounded to the second digit after the decimal point.

Table 3: Summary of the Tevatron combined average M_t . The uncertainty categories are described in the text. The total systematic uncertainty and the total uncertainty are obtained by adding the relevant contributions in quadrature.

March 2013	
Tevatron combined values (GeV/c^2)	
M_t	173.20
In situ light-jet calibration (iJES)	0.36
Response to $b/q/g$ jets (aJES)	0.09
Model for b jets (bJES)	0.11
Out-of-cone correction (cJES)	0.01
Light-jet response (2) (dJES)	0.15
Light-jet response (1) (rJES)	0.16
Lepton modeling (LepPt)	0.05
Signal modeling (Signal)	0.52
Jet modeling (DetMod)	0.08
Offset (UN/MI)	0.00
Background from theory (BGMC)	0.06
Background based on data (BGData)	0.13
Calibration method (Method)	0.06
Multiple interactions model (MHI)	0.07
Systematic uncertainty (Syst)	0.71
Statistical uncertainty (Stat)	0.51
Total uncertainty	0.87

Table 4: The pull and weight for each of the inputs used to determine the Tevatron average mass of the top quark. See Ref. [34] for a discussion of negative weights.

March 2013												
	Run I published					Run II published						Run II preliminary
	CDF			DØ		CDF			DØ			CDF
	ℓ +jets	$\ell\ell$	alljets	ℓ +jets	$\ell\ell$	ℓ +jets	$\ell\ell$	alljets	L_{XY}	ℓ +jets	$\ell\ell$	MEt
Pull	+0.40	-0.51	+1.11	+1.32	-0.38	-0.51	-0.82	-0.41	-0.67	1.42	+0.30	+0.45
Weight [%]	-4.7	-1.1	-0.9	+0.4	-0.2	+62.0	-0.3	+10.5	+0.22	+20.6	+1.4	+11.9

237 correspond to chi-squared probabilities of 25%, 79%, 74%, 52%, 27%, and 66% respectively,
 238 indicating that all decay channels are consistent with one other.

239 In order to test the influence of the correlation choices, we performed a cross-check by
 240 changing all non-diagonal correlation coefficients of the correlation matrix defined in Section 4
 241 from 100% to 50% and re-evaluated the combination. The result from this extreme test is a

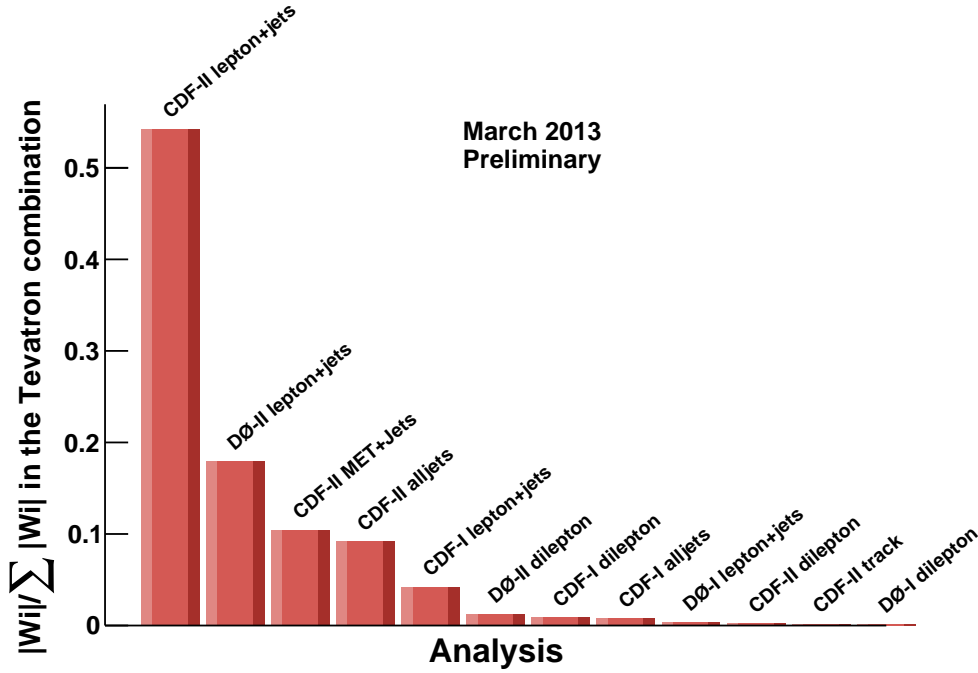


Figure 2: Relative weights of the input measurements in the combination. The relative weights have been obtained by dividing the absolute value of each measurement weight by the sum over all measurements of the absolute values of the weights.

Table 5: Summary of the combination of the 12 measurements by CDF and DØ in terms of four physical quantities, the mass of the top quark in the alljets, ℓ +jets, $\ell\ell$ and MET decay channels.

March 2013					
Parameter	Value (GeV/c^2)	Correlations			
		M_t^{alljets}	M_t^{l+j}	$M_t^{\text{di-l}}$	M_t^{MEt}
M_t^{alljets}	172.7 ± 1.9	1.00			
M_t^{l+j}	173.2 ± 0.9	0.25	1.00		
$M_t^{\text{di-l}}$	170.0 ± 2.1	0.19	0.41	1.00	
M_t^{MEt}	173.8 ± 1.8	0.13	0.26	0.18	1.00

242 0.19 GeV/c^2 shift of the top-quark mass and a 0.03 GeV/c^2 decrease of the total uncertainty.

243 We also performed two separate combinations of all the CDF measurements and all the
 244 DØ ones. The results of these combinations are $172.72 \pm 0.93 \text{ GeV}/c^2$ for CDF and $174.89 \pm$

245 1.42 GeV/ c^2 for $D\bar{O}$. Taking all correlations into account, we calculate the chi-square $\chi^2(CDF -$
246 $D\bar{O}) = 2.25/1$ corresponding to a probability of 13%.

247 6 Summary

248 A preliminary combination of measurements of the mass of the top quark from the Tevatron
249 experiments CDF and $D\bar{O}$ is presented. The combination includes five published Run I measure-
250 ments, six published Run II measurements, and one preliminary Run II measurements. Taking
251 into account the statistical and systematic uncertainties and their correlations, the preliminary
252 result for the Tevatron average is $M_t = 173.20 \pm 0.51$ (stat) ± 0.71 (syst) GeV/ c^2 , where the total
253 uncertainty is obtained assuming Gaussian systematic uncertainties. Adding in quadrature the
254 statistical and systematic uncertainties yields a total uncertainty of 0.87 GeV/ c^2 , correspond-
255 ing to a relative precision of 0.50% on the top-quark mass. Rounding off the uncertainty to
256 two significant digits, the combination yields $M_t = 173.2 \pm 0.9$ GeV/ c^2 . The central value is
257 0.02 GeV/ c^2 higher than our July 2011 average of $M_t = 173.18 \pm 0.94$ GeV/ c^2 .

258 The mass of the top quark is now known with a relative precision of 0.50%, limited by the
259 systematic uncertainties, which are dominated by the jet energy scale uncertainty. This result
260 will be further improved when all analysis channels from CDF and $D\bar{O}$ using the full Run II
261 data set are finalized.

262 7 Acknowledgments

263 We thank the Fermilab staff and the technical staffs of the participating institutions for their
264 vital contributions. This work was supported by DOE and NSF (USA), CONICET and UBA-
265 CyT (Argentina), CNPq, FAPERJ, FAPESP and FUNDUNESP (Brazil), CRC Program, CFI,
266 NSERC and WestGrid Project (Canada), CAS and CNSF (China), Colciencias (Colombia),
267 MSMT and GACR (Czech Republic), Academy of Finland (Finland), CEA and CNRS/IN2P3
268 (France), BMBF and DFG (Germany), Ministry of Education, Culture, Sports, Science and
269 Technology (Japan), World Class University Program, National Research Foundation (Korea),
270 KRF and KOSEF (Korea), DAE and DST (India), SFI (Ireland), INFN (Italy), CONACyT
271 (Mexico), NSC(Republic of China), FASI, Rosatom and RFBR (Russia), Slovak R&D Agency
272 (Slovakia), Ministerio de Ciencia e Innovación, and Programa Consolider-Ingenio 2010 (Spain),
273 The Swedish Research Council (Sweden), Swiss National Science Foundation (Switzerland),
274 FOM (The Netherlands), STFC and the Royal Society (UK), and the A.P. Sloan Foundation
275 (USA).

276 References

- 277 [1] The ATLAS and CMS Collaborations, ATLAS-CONF-2012-095, CMS PAS TOP-12-001
278 (2012), <http://cds.cern.ch/record/1460441/>
- 279 [2] F. Abe *et al.* [CDF Collaboration], Phys. Rev. Lett. **80** (1998) 2779, [hep-ex/9802017](#).
- 280 [3] F. Abe *et al.* [CDF Collaboration], Phys. Rev. Lett. **82** (1999) 271, [hep-ex/9810029](#).
- 281 [4] F. Abe *et al.* [CDF Collaboration], Erratum: Phys. Rev. Lett. **82** (1999) 2808,
282 [hep-ex/9810029](#).
- 283 [5] B. Abbott *et al.* [DØ Collaboration], Phys. Rev. Lett. **80** (1998) 2063, [hep-ex/9706014](#).
- 284 [6] B. Abbott *et al.* [DØ Collaboration], Phys. Rev. **D60** (1999) 052001, [hep-ex/9808029](#).
- 285 [7] F. Abe *et al.* [CDF Collaboration], Phys. Rev. Lett. **80** (1998) 2767, [hep-ex/9801014](#).
- 286 [8] T. Affolder *et al.* [CDF Collaboration], Phys. Rev. **D63** (2001) 032003, [hep-ex/0006028](#).
- 287 [9] S. Abachi *et al.* [DØ Collaboration], Phys. Rev. Lett. **79** (1997) 1197, [hep-ex/9703008](#).
- 288 [10] B. Abbott *et al.* [DØ Collaboration], Phys. Rev. **D58** (1998) 052001, [hep-ex/9801025](#).
- 289 [11] V. M. Abazov *et al.* [DØ Collaboration], Nature **429** (2004) 638, [hep-ex/0406031](#).
- 290 [12] F. Abe *et al.* [CDF Collaboration], Phys. Rev. Lett. **79** (1997) 1992.
- 291 [13] V. M. Abazov *et al.* [DØ Collaboration], Phys. Lett. **B606** (2005) 25, [hep-ex/0410086](#).
- 292 [14] The CDF Collaboration, the DØ Collaboration and the Tevatron Electroweak Working
293 Group, [arXiv:1107.5255](#).
- 294 [15] T. Aaltonen *et al.* [CDF Collaboration], CDF Conference Note 10433.
- 295 [16] T. Aaltonen *et al.* [CDF Collaboration], Phys. Rev. Lett. **107** (2011), 232002.
- 296 [17] T. Aaltonen *et al.* [CDF Collaboration], Phys. Rev. Lett. **109** (2012) 152003.
- 297 [18] T. Aaltonen *et al.* [CDF Collaboration], Phys. Rev. D **81** (2010) 032002, Phys. Rev. D
298 **83** (2011) 111101, [arXiv:1105.0192](#).
- 299 [19] T. Aaltonen *et al.* [CDF Collaboration], Phys. Lett. B **714**, 24 (2012).
- 300 [20] V. M. Abazov *et al.* [DØ Collaboration], Phys. Rev. Lett. **101** (2008) 182001.
301 [arXiv:0807.2141](#).
- 302 [21] V. M. Abazov *et al.* [DØ Collaboration], Phys. Rev. D **84**, (2011), 032004 (2011).

- 303 [22] V. M. Abazov *et al.* [DØ Collaboration], Phys. Rev. D **86**, 051103 (2012).
- 304 [23] T. Aaltonen *et al.* [CDF Collaboration], Phys. Rev. D **81** (2010) 032002.
- 305 [24] T. Aaltonen *et al.* [CDF and DØ Collaboration], Phys. Rev. D **86** (2012) 092003.
- 306 [25] The CDF Collaboration, the DØ Collaboration, and the Tevatron Electroweak Working
307 Group, [hep-ex/0404010](#).
- 308 [26] The CDF Collaboration, the DØ Collaboration, and the Tevatron Electroweak Working
309 Group, [hep-ex/0507091](#).
- 310 [27] The CDF Collaboration, the DØ Collaboration, and the Tevatron Electroweak Working
311 Group, [hep-ex/0603039](#).
- 312 [28] The CDF Collaboration, the DØ Collaboration, and the Tevatron Electroweak Working
313 Group, [hep-ex/0608032](#).
- 314 [29] The CDF Collaboration, the DØ Collaboration, and the Tevatron Electroweak Working
315 Group, [hep-ex/0703034](#).
- 316 [30] The CDF Collaboration, the DØ Collaboration, and the Tevatron Electroweak Working
317 Group, [arXiv:0803.1683](#).
- 318 [31] The CDF Collaboration, the DØ Collaboration, and the Tevatron Electroweak Working
319 Group, [arXiv:0808.1089](#).
- 320 [32] The CDF Collaboration, the DØ Collaboration and the Tevatron Electroweak Working
321 Group, [arXiv:0903.2503](#).
- 322 [33] The CDF Collaboration, the DØ Collaboration and the Tevatron Electroweak Working
323 Group, [arXiv:1007.3178](#).
- 324 [34] L. Lyons, D. Gibaut, and P. Clifford, Nucl. Instrum. Meth. **A270** (1988) 110.
- 325 [35] A. Valassi, Nucl. Instrum. Meth. **A500** (2003) 391.
- 326 [36] V. M. Abazov *et al.* [DØ Collaboration], DØ-note 5900-CONF.
- 327 [37] S. Frixione and B. Webber, JHEP **029** (2002) 0206, [hep-ph/0204244](#).
- 328 [38] M. L. Mangano, M. Moretti, F. Piccinini, R. Pittau, and A. D. Polosa, JHEP **07** (2003)
329 001, [hep-ph/0206293](#).
- 330 [39] G. Marchesini *et al.*, Comput. Phys. Commun. **67** (1992) 465.
- 331 [40] G. Corcella *et al.*, JHEP **01** (2001) 010, [hep-ph/0011363](#).
- 332 [41] P. Z. Skands and D. Wicke, Eur. Phys. J. C **52** (2007) 133 [hep-ph/0703081](#).

- 333 [42] P. Z. Skands, [arXiv:0905.3418](https://arxiv.org/abs/0905.3418).
- 334 [43] H.-U. Bengtsson and T. Sjostrand, *Comput. Phys. Commun.* **46** (1987) 43.
- 335 [44] T. Sjostrand, *Comput. Phys. Commun.* **82** (1994) 74.
- 336 [45] T. Sjostrand *et al.*, *Comput. Phys. Commun.* **135** (2001) 238, [hep-ph/0010017](https://arxiv.org/abs/hep-ph/0010017).
- 337 [46] F. E. Paige and S. D. Protopopescu, BNL Reports 38034 and 38774 (1986) unpublished.